In: Wang, X.; Sauter, U.H.; Ross, R.J., eds. 2019. Proceedings: 21st International Nondestructive Testing and Evaluation of Wood Symposium. General Technical Report FPL-GTR-272. Madison, WI: U.S. Department of Agriculture, Forest Service, Forest Products Laboratory. pp 62-70.

Identifying Incipient Decay in Douglas-fir Bridge Components using X-Ray Computerized Tomography

Christopher Adam Senalik
USDA Forest Service, Forest Products Laboratory, Madison, Wisconsin, USA, christopher.a.senalik@usda.gov

James Wacker
USDA Forest Service, Forest Products Laboratory, Madison, Wisconsin, USA, james.p.wacker@usda.gov

Xiping Wang
USDA Forest Service, Forest Products Laboratory, Madison, Wisconsin, USA, xiping.wang@usda.gov

Xi Wu
School of IoT Engineering, Jiangnan University, Wuxi, Jiangsu, China, xw20170909@gmail.com

Abstract

In this report, wooden members of sizes typically used in bridge construction are examined using x-ray computerized tomography (CT) to determine the presence of internal decay. This report is part of an overall study in which Douglas-fir (*Pseudotsuga menziesii*) glue-laminated (glulam) beams and solid sawn timbers were inoculated with brown rot fungus, *Fomitopsis pinicola*, and exposed to aboveground conditions approximately 25 miles (40 km) north of Gulfport, Mississippi, USA. The goal of the overall study is to develop interior decay within the test specimens and then identify and characterize the decay using a variety of nondestructive testing (NDT) techniques. One NDT technique used is x-ray CT. The pixel brightness (PB) of CT scan images is proportional to the specific gravity (SG) at that location; high SG materials appear brighter whereas low SG materials appear darker. The consumption of wood by fungus decreases the wood SG; however, fungal progression takes place in areas where sufficient moisture is present. The presence of moisture increases wood SG as detected by the CT scan, which masks the effect of the fungal decay, which is a common co-occurrence with many NDT techniques. To identify incipient decay, it is necessary to examine the ring structure both within and outside of the area of moisture. Quantifying the extent of the decay requires correlating the PB to known SG values for both dry wood and wood of varying moisture content. In this report, the relationship between wood SG, moisture content, and PB was quantified.

Keywords: x-ray computerized tomography, wood timber, brown rot fungus, incipient decay

Introduction

Wood attacked by decay fungi often suffers drastic decreases in mechanical properties, which are relied upon for structural soundness. This degradation occurs because the fungus degrades components of the cell wall. Modulus of rupture (MOR), modulus of elasticity (MOE), compression strength, tension strength, toughness, and hardness are among the key properties compromised. The effect of brown rot and white rot fungi on both softwoods and hardwoods is well known. A concise summary of relevant publications was provided in Ross et al. (2018). For a 5% mass loss caused by brown rot, reductions to MOR, MOE, and tension strength parallel to grain can be 50% or more. For this reason, early detection of incipient fungal decay is of paramount importance.

This report is part of an overall study using a variety of nondestructive testing (NDT) techniques to identify the presence of decay in timbers of sizes commonly used in bridge construction. In this report,

Douglas-fir (*Pseudotsuga menziesii*) glue-laminated (glulam) beams and solid sawn timbers were inoculated with brown rot fungus, *Fomitopsis pinicola*, and exposed to aboveground conditions approximately 25 miles (40 km) north of Gulfport, Mississippi, USA. The glulam beams and sawn timbers were of sizes typically used in bridge construction and hereafter are referred to collectively as bridge components. The bridge components were exposed to outdoor weather conditions from periods ranging from 6 to 30 months. A full description of the inspection methods, inoculation process, test setup, schedule of exposure, and postexposure nondestructive assessment can be found in Wacker et al. (2016) and Senalik et al. (2016).

One postexposure technique used, x-ray computerized tomography (CT), is the focus of this report. The use of x-ray CT to examine wood for internal decay is not new. Bucur (2003) described the use of x-ray CT on wood. McGovern et al. (2010) used x-ray CT to assess the amount of internal mass lost on 1-in. (25-mm) cubes of loblolly pine that had been subjected to varying degrees of mass loss from rot. Senalik (2013) evaluated the soundness of wooden utility poles and glulam beams with x-ray CT. However, in the studies conducted by Senalik and McGovern, the wood specimens had a moisture content of 12% or lower.

Moisture within the beams complicates the process of detecting internal decay. Many common forms of wood-attacking fungi require water to grow and thrive; therefore, fungal decay often occurs within moisture pockets. Fungi also produce water as a byproduct of their extracellular digestion process. As fungus progresses through the wood, it deteriorates the wood, leading to mass loss through extracellular digestion of the structural carbohydrates. In a CT scan, the specific gravity (SG) of a location is proportional to the pixel brightness (PB) of that region as it appears on the CT output. Areas of high SG appear bright, whereas areas of low SG appear dark. Wood with high moisture content appears bright, whereas wood that is deteriorated and suffering mass loss will appear dark. Unfortunately, when these two phenomena overlap, the apparent increase in SG from the moisture content can obscure the loss of mass from fungal attack. In this paper, the process of identifying areas of decreased mass within moisture pockets as shown in x-ray CT scans is described.

Materials and Methods

The Douglas-fir bridge components had one of four cross-sectional sizes: 5-1/8- by 9-in. (130- by 229-mm) glulam, 5-1/8- by 7.5-in. (130- by 191-mm) glulam, 3-1/2- by 5-1/2-in. (89- by 140-mm) sawn timber, and 3-1/2- by 7-1/4-in. (89- by 184-mm) sawn timber. Each specimen was 32 in. (0.8 m) in length. For brevity, the figures herein show only 5-1/8- by 9-in. (130- by 229-mm) glulam, but all cross sections were used in the analysis presented in this report. Each specimen was inoculated with brown rot fungus, *Fomitopsis pinicola*, prior to placement for field exposure. Figure 1 shows the specimen configuration. There were eight sets of specimens. Each set contained 12 specimens (three of each cross-sectional size). Each set was subjected to weather exposure in 6-month increments. The first set was exposed for 6 months, the second set was exposed for 12 months, through the final set which was exposed for 30 months. A full description of the specimen preparation and field exposure is given in Senalik et al. (2016). After the field exposure time period was completed, the specimens were shipped back to the Forest Products Laboratory (FPL) in Madison, Wisconsin. The x-ray CT scanning of select beams was performed at the University of Wisconsin, School of Veterinary Medicine, Madison, Wisconsin, using a General Electric Lightspeed Ultra 8-slice helical CT scanner (GE Medical Systems, Milwaukee, Wisconsin, USA).

The x-ray CT energy level and intensity were 120 kV and 120 mA, respectively. CT scanners measure the radiodensity of materials. Radiodensity is the opacity of a material to the radio and x-ray portion of the spectrum. CT scanners express their measurements of radiodensity in terms of a dimensionless unit

known as the Hounsfield unit (HU). For reference, HU values for air, water at standard temperature and pressure, and dense bone are -1,000, 0, and +2,000, respectively. During postprocessing of the images, the width (W) of the HU window was chosen to be 1,500, and the center point of the window, known as the level (L), was set to -300. These values are commonly written shorthand as 1500W, -300L.

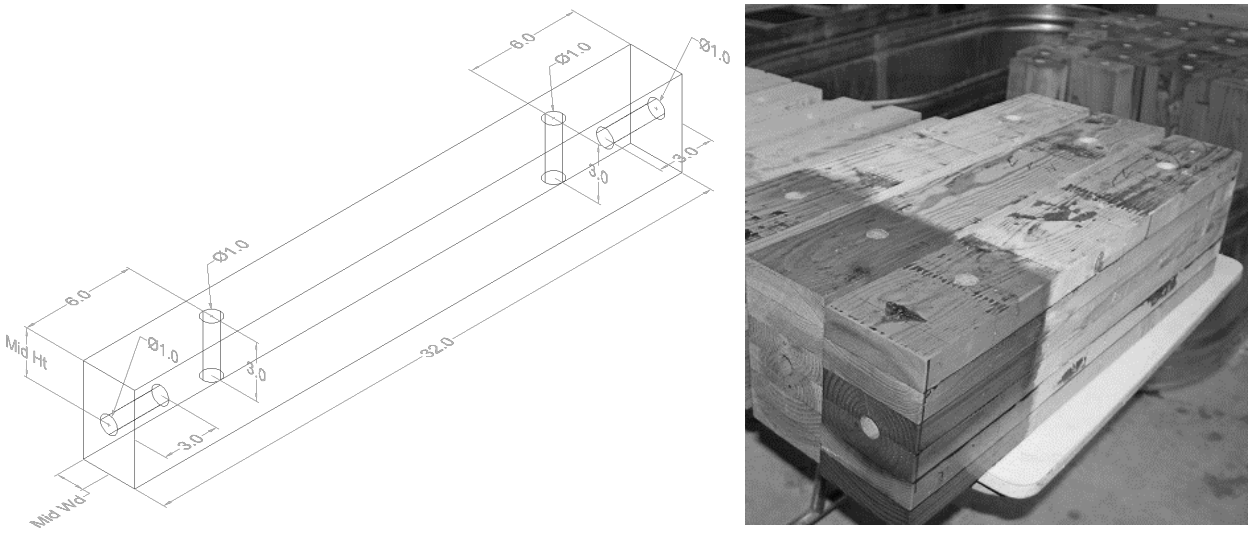

Figure 1—Fungal cavity holes in specimens: (a) locations of drilled holes. Units shown are in inches (1 in. = 25.4 mm); (b) holes drilled in a six-layer glulam.

The width of the window determines the resolution between levels of SG that are apparent in the image. A wider window allows viewing a wider range of densities. A narrow window has as smaller range, but the resolution between levels of SG is sharper. The level is the midpoint of the window. In this report, the level was set to -300 and the window was set at 1,500; therefore, any values above 450 HU (-300 + 1,500/2 = 450) appear as white, and any values below -1,050 (-300 – 1,500/2 = -1,050) appear as black. All values in between appear as some shade of gray. The W and L values are chosen such that decayed low SG wood and moisture-saturated high SG wood fall within the range. It is important to note that HU is not the same as PB. HUs are used to construct the CT scan data file. The CT scan data file is then interpreted using specialized software (in this case, eFilmLite Ver. 4.0 from Merge Healthcare, Chicago, Illinois, USA) which converts the HU value to a PB for display on a computer screen. While the window of the images is 1,500 HU, a normal pixel has a brightness range between 0 (completely black) and 255 (completely white). Therefore, an increase in PB of 1 (say from 121 to 122) encompasses approximately 5.9 HU. An in-depth discussion of HU, CT scanners, and PB displays can be found in Romans (2010). The width and level can be adjusted to accentuate particular SG ranges if desired. It should be remembered that wood is an organic material with variability. It is easy to narrow the window such that small, natural variations in wood SG appear dramatic on the computer screen.

Figure 2 shows three examples of glulam beam CT scans. Figure 2a shows a six-layer glulam after 6 months of exposure. The portion of the beam shown has no visible internal moisture pocket. The ring structure of each lamina is clearly visible. Pith is visible in the third layer from the top (all references to layers will assume the top layer is the first and the bottom is the sixth). The fifth layer contains a small knot. Figure 2b shows the same beam but in a region with a pocket of high moisture. Decay often grows in areas of high moisture, but the brief exposure time limits the likelihood of significant fungal attack. The moisture portion is visible as a bright spot that crosses layers 1 through 3. The tree rings are visible within the moisture region. Figure 2c shows a cross section with a moisture pocket after 24 months of

exposure. It is difficult to tell if there was decreased SG caused by fungal decay within the moisture pocket.

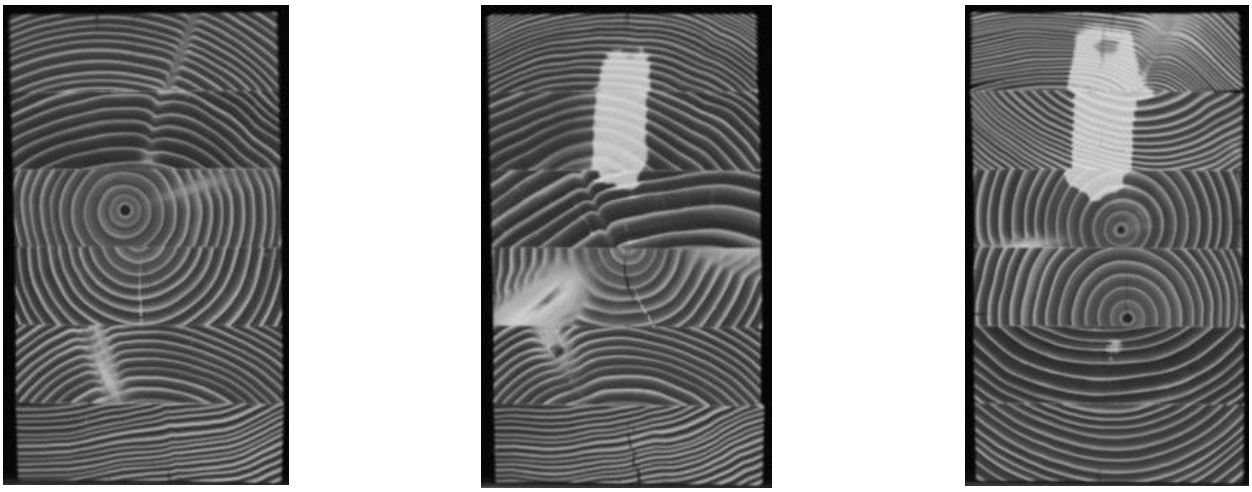

(a) **(b)** **(c)**

Figure 2—X-ray CT scans of six-layer glulam beams. CT settings were energy level of 120 kV and intensity of 120 mA. HU settings were 1,500W and -300L: (a) cross section after 6 months from a portion of the beam devoid of moisture; (b) cross section after 6 months from a portion with moisture; (c) cross section after 24 months with moisture.

To determine a more precise relationship between PB and SG, a set of 24 wood blocks of varying SG were used to develop reference points with the CT scans. SG for the blocks was determined at 12% moisture content. The blocks were mostly low characteristic tropical species; annual rings were nonexistent or barely visible, and knots and pith were avoided. The goal is for each block to be as close to uniform density throughout as possible. Figure 3a shows the blocks held within a container. Figure 3b shows the CT scan of the blocks. The container was placed alongside each beam as it was scanned. The container was stored in a temperature- and humidity-controlled room between uses, which kept the equilibrium moisture content of the wood at 12%. Table 1 identifies the species and SG of each block.

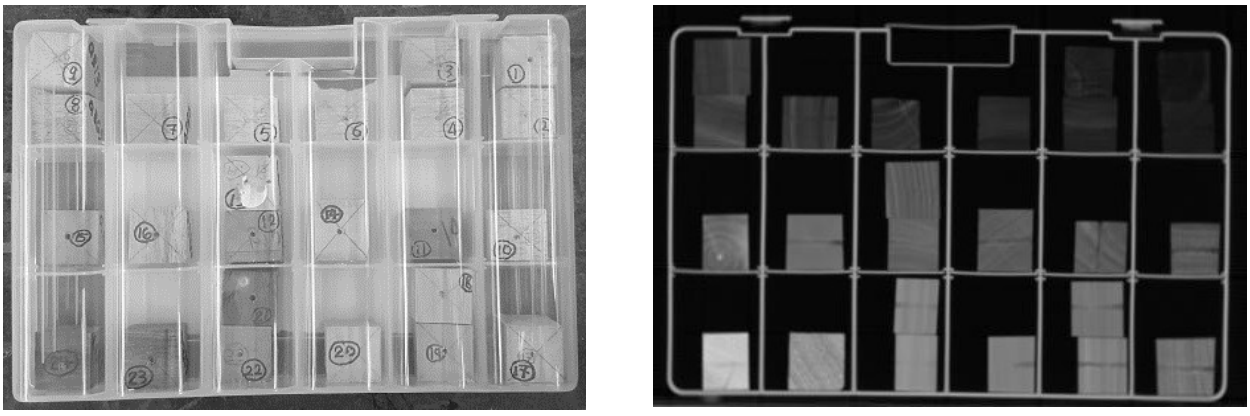

(a) **(b)**

Figure 3—Series of wood blocks used to relate pixel brightness with specific gravity for dry wood: (a) the 24 wood blocks in the container; (b) a CT scan of the wood blocks using the settings given in Figure 1. The range of specific gravity is 0.080 for block 1 (upper right) through 1.121 for block 24 (lower left).

Table 1—Wood specimen identification and specific gravity (SG)

ID	Species	SG	ID	Species	SG
1	*Heliocarpus appendiculatus* Turcz.	0.081	13	*Liquidambar sp.*	0.507
2	*Ochroma pyramidale* (Cav. ex Lam.) Urb.	0.118	12	*Trema micrantha* (L.) Blume	0.561
3	*Ochroma pyramidale* (Cav. ex Lam.) Urb.	0.148	16	*Mangifera sp.*	0.580
4	*Ochroma pyramidale* (Cav. ex Lam.) Urb.	0.180	15	*Alnus sp.*	0.610
6	*Ochroma pyramidale* (Cav. ex Lam.) Urb.	0.194	17	*Gonystylus sp.*	0.624
5	*Hampea Appendiculata* (Donn. Sm.) Standl.	0.226	18	*Betula sp.*	0.648
7	*Ochroma pyramidale* (Cav. ex Lam.) Urb.	0.287	19	*Nyssa*	0.693
9	*Ochroma pyramidale* (Cav. ex Lam.) Urb.	0.313	20	*Nyssa*	0.707
8	*Ochroma pyramidale* (Cav. ex Lam.) Urb.	0.364	21	*Julbernardia sp.*	0.732
10	*Hampea appendiculate* (Donn. Sm.) Standl.	0.468	22	*Laetia procera* (Poepp.) Eichl.	0.801
11	*Trema micrantha* (L.) Blume	0.493	23	*Shorea sp.*	0.833
14	*Laurelia sp.*	0.504	24	*Chrysophyllum sp.*	1.121

Several of the blocks in Table 1 are of the same species. For example, *Ochroma pyramidale* (Cav. ex Lam.) Urb., commonly known as balsa wood, has seven entries. Balsa wood can have a range of SG from approximately 0.10 to 0.35. Personnel from the Center for Wood Anatomy Research at FPL identified a set of wood samples with SG from 0.08 to 1.121. This range should encompass any SG value likely to be encountered during the project. The container itself is constructed of high-density polyethylene (HDPE), which has an SG of between 0.93 and 0.97. The SG of the container is distinct from any of the blocks and easily removed from calculations. The PB assigned to each block is the average PB across all visible pixels. Edge pixels for each block were not used in the calculations as their brightness can be influenced by the density of surrounding materials (air, HDPE, etc.).

To determine if the presence of moisture pockets exhibits nonlinear effects on the x-ray CT scan, a separate set of tests was conducted. Figure 4 shows fifteen 1-in. (25.4-mm) cubed wood blocks of Douglas-fir, which were cut from remnants of the sawn timbers used in the overall decay study. The blocks were soaked in water and then removed at different intervals prior to the CT scan to obtain the range of moisture contents. The blocks were weighed prior to and just after the CT scan, and all dimensions were measured. The blocks were then oven-dried to determine the dry weight of the wood alone. PB was determined in the same manner as those in Figure 3.

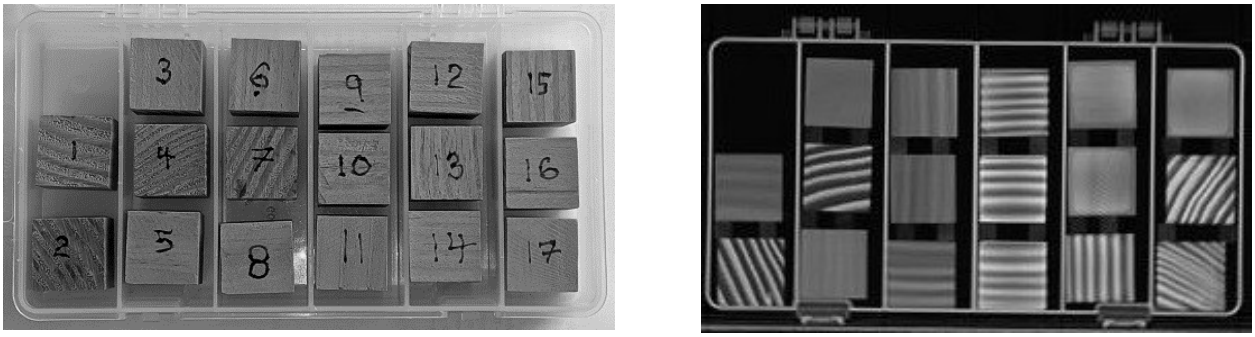

a. **b.**

Figure 4—Series of wood blocks used to relate pixel brightness with specific gravity for wet wood: (a) the 17 wood blocks in the container; (b) a computerized tomography scan of the wood blocks using the settings given in Figure 1.

Discussion and Results

Figure 5 shows the relationship between PB and SG for both the dry and wet wood blocks. The dry wood blocks were used in 24 separate CT scans; the wet wood blocks were used in eight separate CT scans. Values from all CT scans are shown in Figure 5. Although the SG for each block does not change, the PB can vary slightly depending upon inconsistencies in the wood blocks themselves and minor differences in positioning of the blocks. Below each figure is the linear equation relating PB to SG. The equations yield SG values within 2% of each other for PB values of 50 or greater (SG of 0.3 or greater).

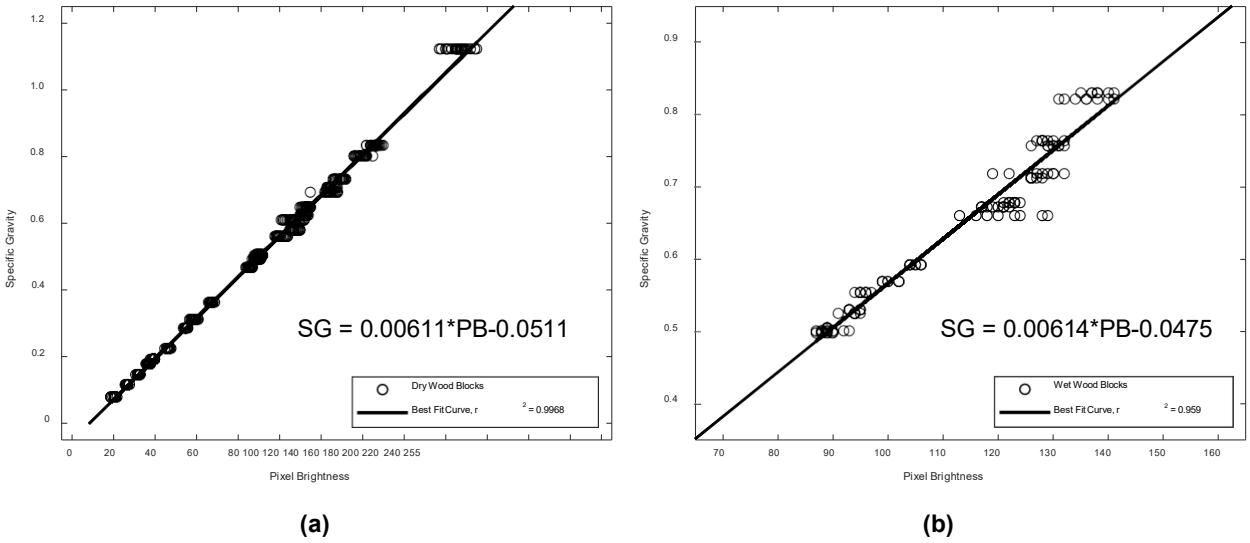

Figure 5—Relationships between pixel brightness (PB) of x-ray CT scans and specific gravity (SG). CT scan settings match those given in Figure 1: (a) dry wood; (b) wet wood.

In Figure 6, all data points from Figures 5a and 5b are shown on a single chart. The equation for the combined data set is shown below the figure. The equation yields SG values with 1.5% of the wet and dry wood equations given in Figure 5 for a PB range of 50 or greater (SG of 0.3 or greater).

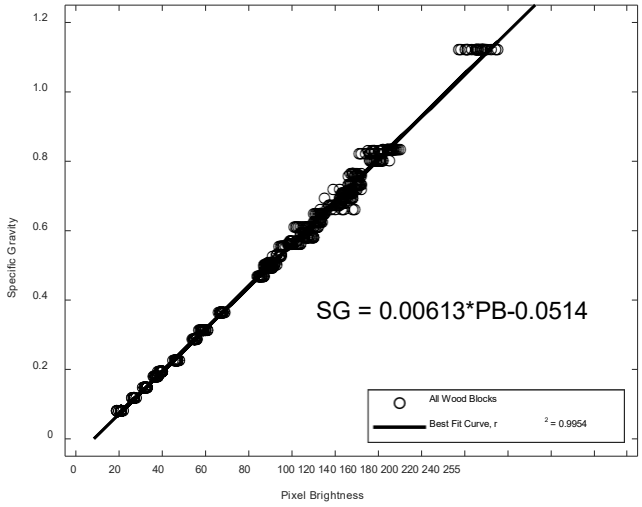

Figure 6—Relationships between pixel brightness (PB) of x-ray CT scans and specific gravity (SG) for all wood blocks. CT scan settings match those given in Figure 1.

Based upon the small percentage difference in values calculated using the relationship developed between PB and SG for dry wood and wet wood shown in Figures 5 and 6, it is reasonable to assume that, if water does create nonlinear effects, then those effects are minimal and inconsequential across the range examined. With this confirmation, the examination of the moisture regions for signs of decay can begin. It is important to note that these equations are developed for the HU settings of 1,500W and -300L. Changing these settings would change the relating equation.

The histogram in Figure 7a shows the number of occurrences of PB within the moisture region of lamina 2, as well as a dry region that is probably devoid of decay, for the cross section shown in Figure 2b (6 months of exposure). The regions in question are shown surrounded by white boxes in Figure 7b. The moisture region is surrounded by a dashed line box; the dry region is surrounded by a solid line box. The portion of the dry region histogram extending from the lowest brightness peak to the first occurrence of zero pixels for a brightness value is assumed to be the normal brightness range for the lowest density earlywood that is devoid of decay. A region of the same width is then put onto the histogram of the wet region. Any pixels that have brightness values below the range may be indicative of the presence of rot. Only two pixels of 1,250, or 0.24%, fell below the range, indicating that it is unlikely that decay was present.

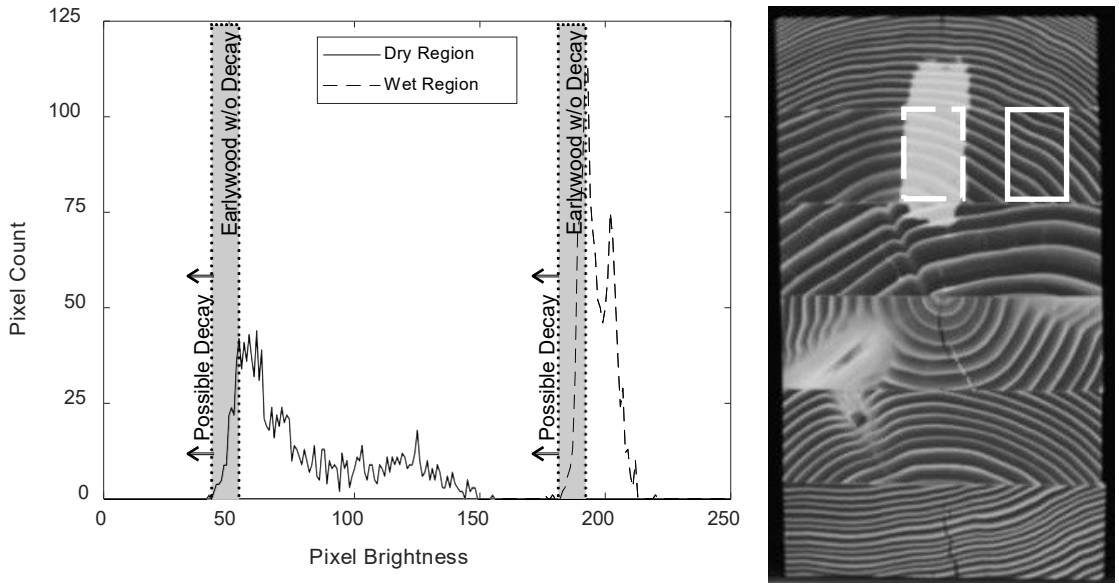

Figure 7—Data from a bridge component that was exposed for 6 months: (a) pixel brightness distribution for the second glulam layer for a region of moisture and a dry region. The gray region on the solid line encompasses the range of earlywood pixel brightness for a region believed to be devoid of decay. A region of the same width is shown on the wet region. Pixels with brightness below the region may indicate presence of decay. Pixels that fall below the region make up 0.24% of the total pixels in the moisture region, indicating that it is unlikely decay is present; (b) cross section of a glulam exposed for 6 months (as shown in Figure 2b). The dashed line box surrounds pixels used for the wet region of Figure 7a; the solid line box surrounds pixels used for the dry region of Figure 7a.

The same procedure was carried out for the glulam beam that was exposed to weather for 24 months. Figure 8a shows the number of occurrences of PB within the moisture region of lamina 2 as well as a dry region that is probably devoid of decay for the cross section shown in Figure 2c (24 months of exposure). The regions in question are shown surrounded by white boxes in Figure 7b. The moisture region is

surrounded by a dashed line box; the dry region is surrounded by a solid line box. The portion of the dry region histogram extending from the lowest peak to the first occurrence of zero pixels for a brightness value was assumed to be the normal brightness range for the earlywood in that lamina of the beam. A region of the same width is then put onto the histogram of the wet region. Any pixels with brightness values below the range may be indicative of the presence of rot. For the 24-month exposed cross section, 45 of 2,145 pixels, or 2.1%, fell below the range, indicating that decay may have been present. Pixels that fall below the assumed normal range in Figure 8a are shown in black. In Figure 8b, the location of the low brightness (and therefore, low SG) pixels are shown in black. The low SG cannot be explained as splits or ring shake in the area. The NDT techniques used during postprocessing of the beams focus on this and similarly darkened areas as potential locations of decay. As a final step in the examination process, the beam was cut across the cross section and Janka hardness tests were performed. Hardness correlates well with strength (Green et al. 2006) and is severely decreased by the presence of fungal decay. The hardness should provide verification of whether the apparent decrease was caused by fungal decay.

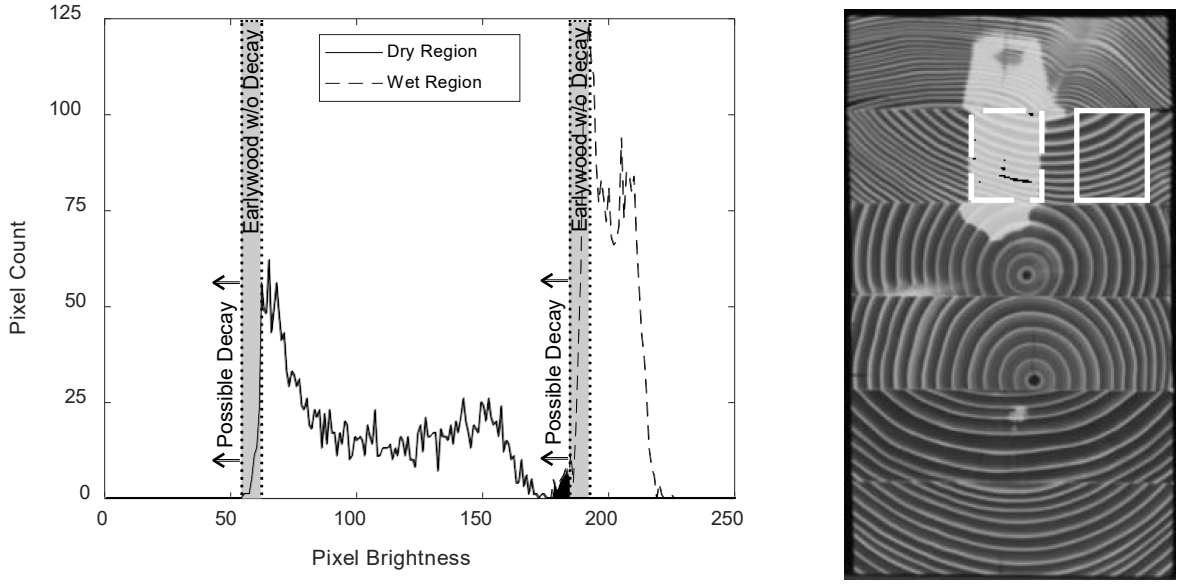

Figure 8—Data from a bridge component that was exposed for 24 months: (a) pixel brightness distribution for the second glulam layer for a region of moisture and a dry region. The gray region on the solid line encompasses the range of earlywood pixel brightness for a region believed to be devoid of decay. A region of the same width is shown on the wet region. Pixels with brightness values below the region may indicate presence of decay. Pixels that fall below the region make up 2.1% of the total pixels in the moisture region, indicating that decay may be starting to develop. The low brightness pixels are shown in the black region; **(b)** cross section of a glulam exposed for 24 months to weather (as shown in Figure 2c). The dashed line box surrounds pixels used for the wet region of Figure 8a; the solid line box surrounds pixels used for the dry region of Figure 8a. The pixels that may indicate the presence of decay are marked in black within the moisture region.

Conclusions

Density increases caused by the presence of moisture can mask the density loss caused by fungal decay. In this paper, a method of finding probable areas of decayed wood within moisture pockets shown in x-ray CT scans of the cross section is described. A linear relationship between PB and SG was developed. The relationship was found to be valid for both wet and dry wood. A threshold of 5% reduction of SG was assumed to be an indicator of the presence of fungal decay. Based upon the assumed threshold, a CT scan from a timber beam exposed to outdoor conditions for 24 months was found to have characteristics

shared with decayed wood. Future examination of the beam should focus on the areas identified using the method described here.

Acknowledgments

This study was conducted under a joint agreement between the Federal Highway Administration (FHWA) – Turner–Fairbank Highway Research Center and the USDA Forest Service, Forest Products Laboratory (FPL). The study was part of the Research, Technology, and Education portion of the National Historic Covered Bridge Preservation (NHCBP) program administered by the FHWA. The NHCBP program includes preservation, rehabilitation, and restoration of covered bridges that are listed or are eligible for listing on the National Register of Historic Places, research for better means of restoring and protecting these bridges, development of educational aids, and technology transfer to disseminate information on covered bridges in order to preserve the Nation's cultural heritage. Michael C. Wiemann of the Center for Wood Anatomy Research at FPL identified species of wood to use in the wood-based image phantom described in Figure 2 and Table 1.

References

Bucur, V. 2003. Nondestructive characterization and imaging of wood. Berlin Heidelberg New York: Springer.

Green, D.W.; Begel, M.; Nelson, W. 2006. Janka hardness using nonstandard specimens. Research Note FPL-RN-0303. Madison, WI: U.S. Department of Agriculture, Forest Service, Forest Products Laboratory. 13 p.

McGovern, M.; Senalik, A.; Chen, G.; Beall, F.; Reis, H. 2010. Detection and assessment of wood decay using x-ray computer tomography. In: Proceedings SPIE Smart Structures/NDE/Sensors and Smart Structures Technologies for Civil, Mechanical, and Aerospace Systems Conference. Paper number 7647-152. San Diego, CA. DOI: 10.1117/12.843709.

Romans, L.E. 2010. Computed tomography for technologists: a comprehensive text, 1st ed. Baltimore, MD: Lippincott Williams & Wilkins.

Ross, R.J.; Wang, X.; Senalik, C.A. 2018. Nondestructive assessment of wood members in a viewing tower in Potawatomi State Park, Door County, Wisconsin, USA. Res. Note FPL-RN-0366. Madison, WI: U.S. Department of Agriculture, Forest Service, Forest Products Laboratory. 14 p.

Senalik, C. 2013. Detection and assessment of wood decay – glulam beams and wooden utility poles. University of Illinois Urbana-Champaign. Doctoral thesis. http://hdl.handle.net/2142/44281.
Senalik, C.A.; Wacker, J.P.; Wang, X.; Jalinoos, F. 2016. Assessing the ability of ground-penetrating radar to detect fungal decay in Douglas-fir beams. In: 25th ASNT research symposium: summaries and abstracts. New Orleans. Columbus, OH: American Society for Nondestructive Testing, Inc.: 110-116.

Wacker, J.P.; Senalik, C.A.; Wang, X.; Jalinoos, F. 2016. Effectiveness of several NDE technologies in detecting moisture pockets and artificial defects in sawn timber and glulam. In: world conference on timer engineering, WCTE 2016. 22-25 August 2016; Vienna, Austria.